




OPEN

# Shifts in regional water availability due to global tree restoration

Anne J. Hoek van Dijke <sup>1,2,3</sup> ✉, Martin Herold <sup>2,4</sup>, Kaniska Mallick<sup>1</sup>, Imme Benedict <sup>5</sup>,  
Miriam Machwitz<sup>1</sup>, Martin Schlerf<sup>1</sup>, Agnes Pranindita<sup>6,7</sup>, Jolanda J. E. Theeuwen <sup>8,9</sup>,  
Jean-François Bastin<sup>10</sup> and Adriaan J. Teuling <sup>3</sup> ✉

**Tree restoration is an effective way to store atmospheric carbon and mitigate climate change. However, large-scale tree-cover expansion has long been known to increase evaporation, leading to reduced local water availability and streamflow. More recent studies suggest that increased precipitation, through enhanced atmospheric moisture recycling, can offset this effect. Here we calculate how 900 million hectares of global tree restoration would impact evaporation and precipitation using an ensemble of data-driven Budyko models and the UTrack moisture recycling dataset. We show that the combined effects of directly enhanced evaporation and indirectly enhanced precipitation create complex patterns of shifting water availability. Large-scale tree-cover expansion can increase water availability by up to 6% in some regions, while decreasing it by up to 38% in others. There is a divergent impact on large river basins: some rivers could lose 6% of their streamflow due to enhanced evaporation, while for other rivers, the greater evaporation is counterbalanced by more moisture recycling. Several so-called hot spots for forest restoration could lose water, including regions that are already facing water scarcity today. Tree restoration significantly shifts terrestrial water fluxes, and we emphasize that future tree-restoration strategies should consider these hydrological effects.**

In June 2021, the United Nations declared the Decade on Ecosystem Restoration to prevent, halt and reverse the degradation of ecosystems worldwide. Large-scale tree restoration is key in climate change mitigation and for enhancing and protecting biodiversity and ecosystem services<sup>1</sup>. Under the current climate conditions, it is estimated that an additional 900 million hectares of tree cover could exist on Earth's surface<sup>2</sup> without encroaching on agriculture and urban areas. During the past decade, numerous global and regional initiatives were initiated to increase tree cover, and this will play an important role in shaping global land use over the next decades. Despite these ongoing initiatives and the claims that ecosystem restoration is beneficial to all of the Sustainable Development Goals<sup>3</sup>, the impact of tree planting on the water cycle and water availability is still poorly understood<sup>4,5</sup>. As a result, potential impacts of ecosystem restoration on ensuring water availability both downstream and downwind are often overlooked.

Tree-cover expansion impacts water availability locally through its effects on the radiation balance, infiltration and soil water storage, evaporation, streamflow and precipitation<sup>6</sup>. Traditionally, local impacts of forest cover on streamflow have been investigated mainly using a so-called paired catchment approach. These studies compare two nearby headwater catchments with similar characteristics over a prolonged period, during which one of the catchments underwent land-cover change while the other did not undergo change. These observational studies have, virtually without exception, concluded that tree planting increases annual evaporation and decreases streamflow<sup>7–12</sup>. This high evaporation is attributed

to the deeper roots of trees (facilitating access to water during dry periods), higher leaf area index (increasing the precipitation interception and canopy conductance), lower snow-free albedo (increasing the energy available for evaporation) and higher aerodynamic roughness (facilitating turbulent exchange) compared with the other vegetation types<sup>9</sup>. Higher evaporation has been reported across different climate zones and tree species, but the magnitude of evaporation differs with climate, tree species and tree age<sup>7,8</sup>. From these studies, it was predicted that large-scale tree restoration will decrease annual mean water availability and streamflow locally<sup>9,13–15</sup>.

In contrast to these small-scale river-basin studies, more recent, large-scale research suggests that the impacts of tree restoration on streamflow are more complex<sup>4,6,16–19</sup>. Through atmospheric feedbacks and transport, the increased evaporation from restored trees will partly recycle back to the terrestrial surface (via so-called evaporation or moisture recycling) and thereby potentially increase downwind rainfall and water availability. Such effects of tree-cover change can reach far beyond the river basin or even continental level: tree-cover change in the Amazon forest could impact precipitation in Canada, Northern Europe and all the way into Eastern Asia<sup>20</sup>. A host of regional and global-scale research has integrated the effects of evaporation recycling in land-cover change studies<sup>4,19,21,22</sup>. These studies have shown that evaporation recycling has a major influence on the water availability and that evaporation recycling should be considered in future land-cover change studies.

No study has quantified the effects of large-scale global tree restoration on water availability by accounting for both the local, direct

<sup>1</sup>Remote Sensing and Natural Resources Modelling Group, ERIN Department, Luxembourg Institute of Science and Technology (LIST), Belvaux, Luxembourg. <sup>2</sup>Laboratory of Geo-Information Science and Remote Sensing, Wageningen University & Research, Wageningen, the Netherlands. <sup>3</sup>Hydrology and Quantitative Water Management Group, Wageningen University & Research, Wageningen, the Netherlands. <sup>4</sup>Helmholtz GFZ German Research Centre for Geosciences, Remote Sensing and Geoinformatics, Telegrafenberg, Potsdam, Germany. <sup>5</sup>Meteorology and Air Quality Group, Wageningen University & Research, Wageningen, the Netherlands. <sup>6</sup>Stockholm Resilience Centre, Stockholm University, Stockholm, Sweden. <sup>7</sup>Bolin Centre for Climate Research, Stockholm University, Stockholm, Sweden. <sup>8</sup>Copernicus Institute of Sustainable Development, Utrecht University, Utrecht, the Netherlands. <sup>9</sup>Wetsus, European Centre of Excellence for Sustainable Water Technology, Leeuwarden, the Netherlands. <sup>10</sup>TERRA Teaching and Research Centre, Gembloux Agro-Bio Tech, University of Liège, Gembloux, Belgium. ✉e-mail: [annehvd@bgc-jena.mpg.de](mailto:annehvd@bgc-jena.mpg.de); [ryan.teuling@wur.nl](mailto:ryan.teuling@wur.nl)

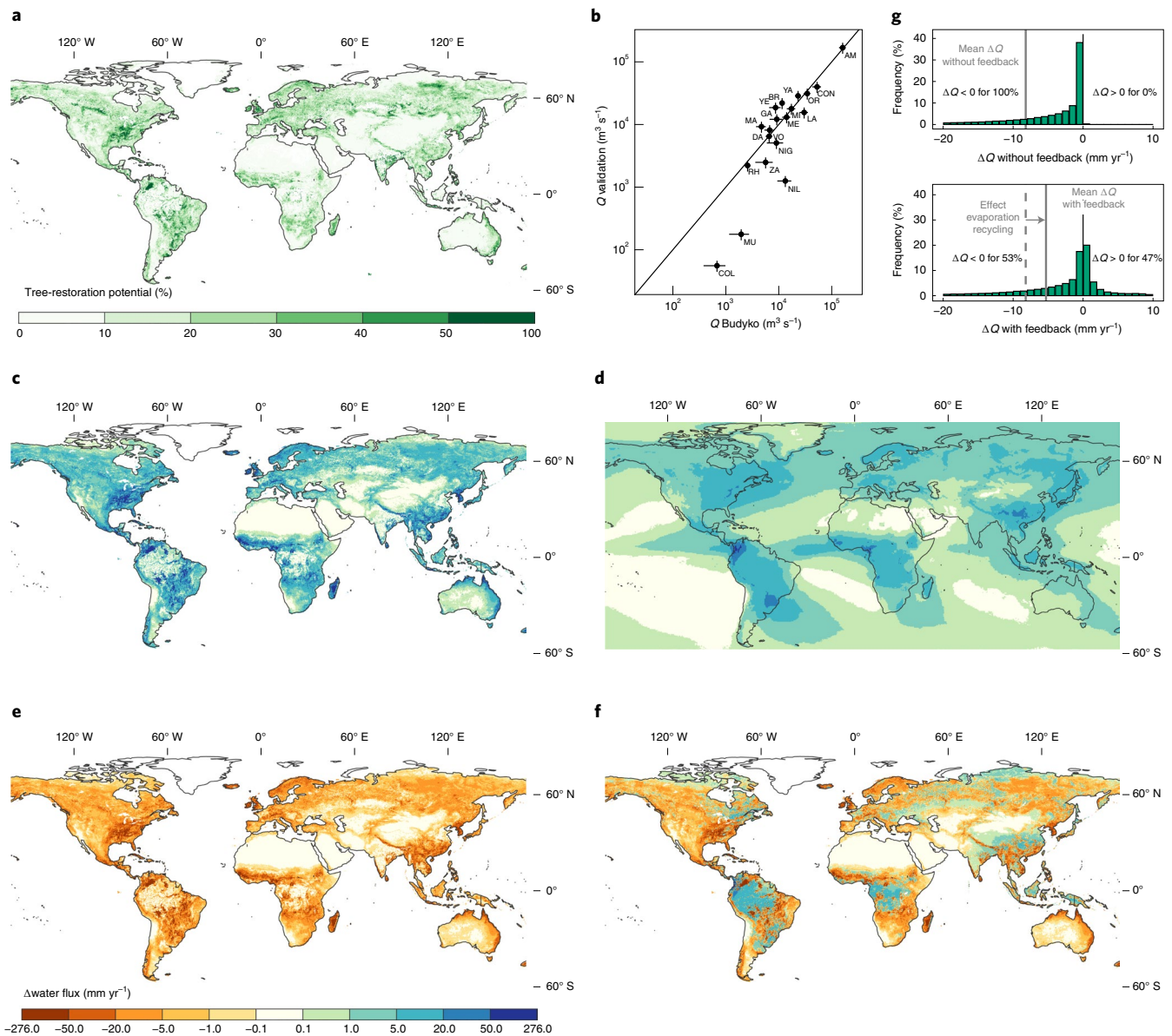


**Fig. 1 | Impacts of forest restoration on water fluxes and water availability.** **a**, The tree-restoration potential<sup>2</sup>: the percentage area of each pixel that is suitable for tree restoration. **b**, Model ensemble mean versus observed streamflow ( $Q$ ) measurements<sup>30</sup> for 19 validated river basins. The error bars for  $Q_{\text{Budyko}}$  indicate the standard deviation over the six Budyko models. The error bars for  $Q_{\text{validation}}$  indicate a 20% error. The river basins are Amazon (AM), Brahmaputra (BR), Colorado (COL), Congo (CON), Danube (DA), Ganges (GA), La Plata (LA), Mackenzie (MA), Mekong (ME), Mississippi (MI), Murray-Darling (MU), Niger (NIG), Nile (NIL), Orinoco (OR), Rhine (RH), Volga (VO), Yangtze (YA), Yenisei (YE) and Zambezi (ZA). **c-f**, The absolute annual change in water fluxes after tree restoration: change in evaporation (**c**), precipitation (**d**), water availability without evaporation recycling (**e**) and water availability with evaporation recycling (**f**). Note that **e** is the inverse of **c**: without the feedback of evaporation recycling, the local increase in evaporation equals the local decrease in water availability. **g**, The histogram shows the distribution of the global changes in water availability without and with evaporation recycling; 89% (without recycling) and 91% (with recycling) of the data fall within the displayed range of  $-20 \text{ mm yr}^{-1}$  to  $+10 \text{ mm yr}^{-1}$ . All maps display the  $0.1^\circ$  mean values, except for **c**, which displays the  $0.5^\circ$  mean value.

effect of increased evaporation and the large-scale, indirect effect of evaporation recycling. The recently published datasets of the 'global tree-restoration potential'<sup>2</sup> and evaporation recycling<sup>23</sup> open up an emerging opportunity for such analyses. In our idealized study, we calculate how large-scale tree restoration (defined as increasing tree cover in any region, independent of the land-use history) influences water availability (defined as precipitation water that is not lost through evaporation, the total water available for consumption, on a yearly basis) and streamflow (the amount of water flowing in a stream; in this study, the accumulation of the as-defined water availability on the river-basin scale). More precisely, we calculate how

a recent estimate of the global tree-restoration potential<sup>2</sup> (Fig. 1a) would impact the fluxes of evaporation, precipitation and streamflow. The global tree-restoration potential dataset highlights where more trees could naturally grow without encroaching on agricultural and urban land. To determine how tree-restoration impacts the long-term partitioning of precipitation between evaporation and streamflow, we use an ensemble of six data-driven Budyko models available in the literature. These six models all include a vegetation parameter that was calibrated separately for forest and non-forest conditions at a 1 km spatial resolution<sup>11,24–27</sup> (Extended Data Fig. 1 and Extended Data Table 1 and 2). We validated the

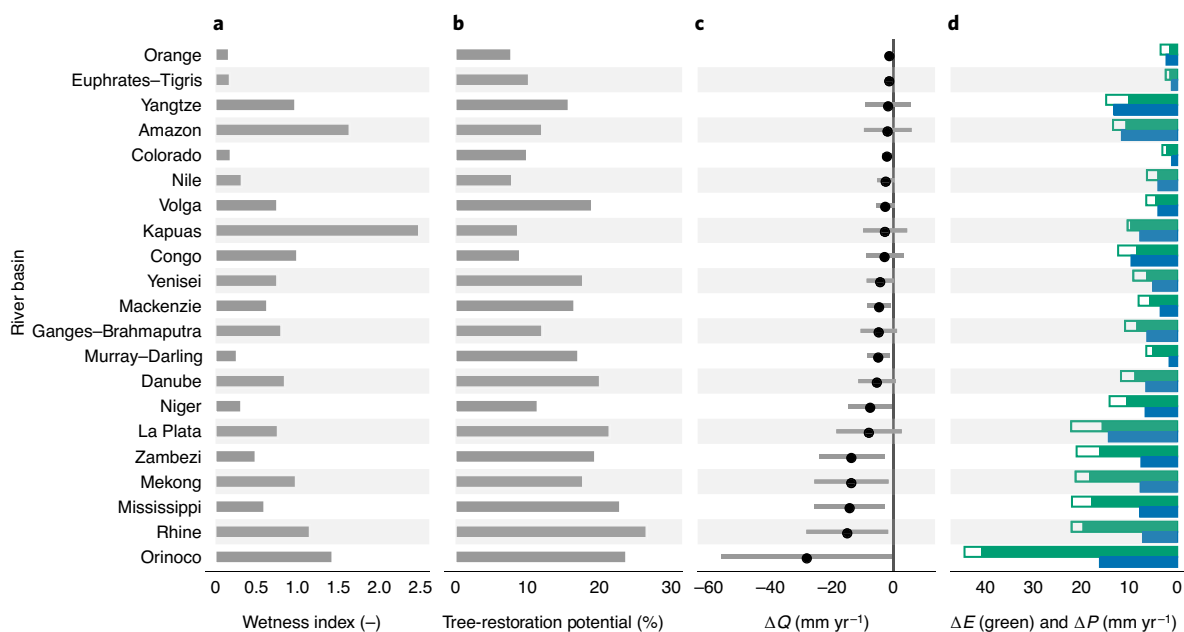


**Fig. 2 | Impacts of global tree restoration on hydrological fluxes in selected river basins. a, b**, Mean wetness index (ratio of precipitation to potential evaporation; **a**) and tree-restoration potential (**b**) for each river basin. **c**, The change in streamflow ( $\Delta Q$ ) with evaporation recycling. The dots indicate the mean river-basin change in streamflow, and the bars indicate one standard deviation (the variation over the six Budyko models). **d**, The change in evaporation ( $\Delta E$ , in green) and precipitation ( $\Delta P$ , in blue). The green bar indicates the increase in evaporation without evaporation recycling, and the green line indicates the increase in evaporation with evaporation recycling (the increase in evaporation when taking into account the increased precipitation). The river basins are sorted from the lowest to the highest decrease in streamflow. The river-basin boundaries are taken from ref. <sup>31</sup>.

multimodel streamflow under current climate and forest-cover conditions against large river-basin run-off (Fig. 1b). We found good agreement over orders of magnitude, except for the Murray–Darling and Colorado basins, where water extraction probably causes the models to overestimate observed run-off. In addition to the Budyko models, we use the recent UTrack dataset of global evaporation recycling<sup>23,28</sup> to calculate where, and to what extent, the increased evaporation could increase (downwind) precipitation. This dataset is created using a state-of-the-art Lagrangian moisture-tracking model<sup>29</sup> and presents the monthly climatological mean evaporation recycling (Extended Data Fig. 2). We assume that tree restoration would intensify the current evaporation-recycling patterns as presented in the UTrack dataset. This approach focuses on the regional distribution of evaporated water but does not consider the effect that land-cover change has on local precipitation or atmospheric circulation and recycling patterns. These assumptions are further addressed in the discussion.

### Impact on water fluxes

Under the current precipitation and potential evaporation, large-scale tree restoration would lead to a direct local increase in terrestrial evaporation of on average  $8.2 \pm 5.5 \text{ mm yr}^{-1}$ , which is an increase of 1.2% (Fig. 1c, Extended Data Fig. 3). The standard deviation characterizes the variation over the six Budyko models. The sign of the average evaporation effect is clear, but the underlying distribution is heavily skewed, and the direct increase in evaporation can exceed  $250 \text{ mm yr}^{-1}$  in the South American tropical forest. When we include the indirect effects of increased evaporation on the atmospheric moisture content and precipitation, we find that 68% of this extra evaporated water would rain out over land (Fig. 1d). Following tree restoration, terrestrial precipitation would increase, with  $4.8 \pm 3.1 \text{ mm yr}^{-1}$  on average due to recycling of increased evaporation (an average increase of 0.7%). While the patterns in the direct evaporation effect are determined by the patterns in tree restoration and local climate, the indirect evaporation-recycling effect

of tree restoration on precipitation happens at the continental scale and is determined by atmospheric circulation.

Without the effect of evaporation recycling, global mean water availability would decrease by  $8.2 \pm 5.3 \text{ mm yr}^{-1}$  (Fig. 1e). When we include the process of evaporation recycling on the water budget calculations (thus taking into account that the evaporated water will partly rain out over land), water availability would decrease by  $5.3 \pm 5.6 \text{ mm yr}^{-1}$  (Fig. 1f). There is, however, a large spatial variability, with regions showing a decreasing (up to 38%) or increasing (up to 6%) water availability (Extended Data Fig. 3). The United Kingdom, for example, has a high tree-restoration potential and therefore a high increase in evaporation. There is, however, low evaporation recycling due to the dominant westerly moisture transport from the country towards Eurasia and due to a low tree-restoration potential upwind in the Atlantic Ocean. Therefore, streamflow in the United Kingdom will decrease more substantially compared with the other regions. The low latitudes and the Tibetan Plateau, however, show an increase in water availability. In these regions, local evaporation recycling is high, for example, due to strong convection above the tropical forest or strong orographic lift in the mountainous regions, and travel distances of the atmospheric moisture are relatively short<sup>28,32</sup>. The results suggest that for half of Earth's surface (47%), the indirect moisture recycling effects of large-scale tree restoration could offset the direct evaporation effects, thus resulting in slight increases in water availability rather than decreases (Fig. 1g).

### Varying effects on streamflow

To evaluate the impacts of tree restoration at the river-basin scale, we aggregate the direct effects (via increased evaporation) and indirect effects (through increased precipitation) for 21 large river basins. For all the river basins, enhanced evaporation reduces streamflow (up to 9%), but streamflow reduction can be close to zero, when increasing precipitation outweighs the increasing evaporation (Fig. 2 and Extended Data Table 3).

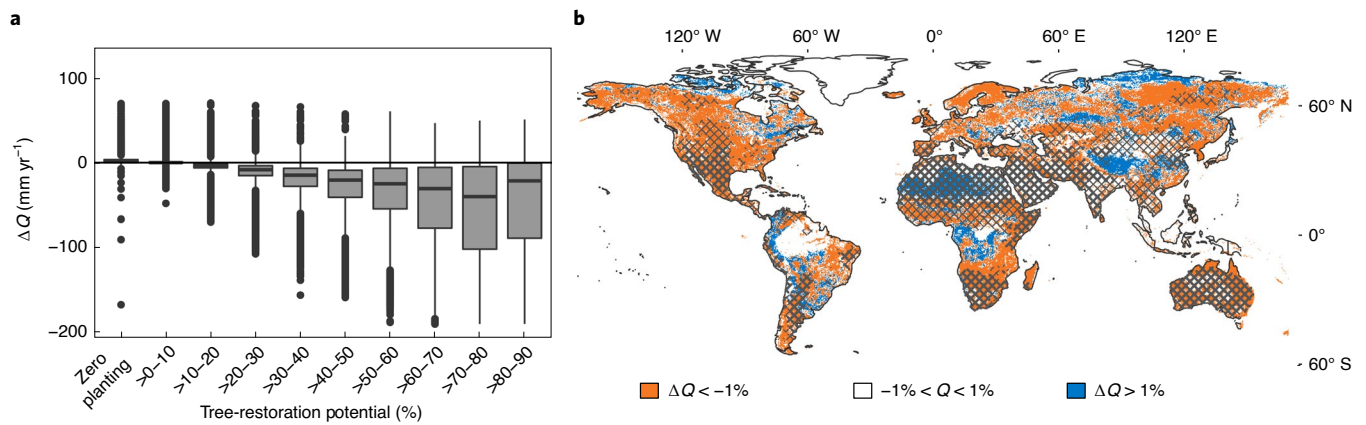


**Fig. 3 | Implications of the percentage restored area and the implications for water scarcity. a**, Water availability could decrease in ‘hot spots for tree restoration’. The lower, middle and upper boundaries of the boxes display the 25th, 50th and 75th percentiles of the data (the interquartile range), respectively. The lines extend to a maximum of 1.5 times the interquartile range. **b**, Water availability will decrease in several regions that currently face water scarcity: the colour indicates whether local water availability will decrease (orange) or increase (blue) following the studied tree-restoration scenario. The cross-hatched regions currently face freshwater scarcity for at least three months per year, and the bold hatched regions face freshwater scarcity for at least nine months per year<sup>34</sup>. Note that we quantified the change in water availability on an annual timescale. The sign of change could vary seasonally, and water availability could, for example, decrease on a yearly basis but remain equal, or even increase, in the dry season.

The increased precipitation is a combination of local recycling (when evaporated water rains out within the same river basin) and recycling of water from other, further upwind, regions. For several tropical basins with a high local evaporation recycling, the high recycling nearly completely compensates for the loss of water through evaporation. Most river basins with a low wetness index (water-limited basins) have a low tree-restoration potential simply because arid regions can only support tree growth if there is significant groundwater convergence<sup>33</sup>. These arid river basins have a small absolute change in evaporation and precipitation. Overall, following tree restoration, streamflow will decrease for most of the world’s important river basins despite the indirect effect of evaporation recycling.

### Implications for water availability

Our study shows that large-scale tree restoration will shift water availability regionally. The hot spots for forest restoration could face a strong reduction in the water availability (Fig. 3a) because water supply by evaporation recycling is not enough to compensate for water loss through evaporation. However, regions with no or limited tree-restoration potential could see an increase in water availability due to the lateral transport of evaporated water into the region. This shows the importance of proper strategic planning of forest restoration projects<sup>35</sup>. Forest restoration could locally enhance precipitation through land–atmosphere interactions<sup>18</sup>, but these effects are complex and not included in our calculations. This enhanced precipitation could partly offset the high water loss in regions with high tree restoration.

Another important finding is that this tree-restoration scenario could further decrease annual water availability in several regions that are already facing water scarcity (Fig. 3b). Rainfall supply for some of these regions is largely of oceanic origin<sup>28,36</sup>, and these regions, therefore, do not, or only to a small extent, see an increase in precipitation after restoration. However, this tree-restoration scenario has the potential to increase water availability in other currently water-scarce regions. Although several regions could see a decrease in annually aggregated water availability, local water availability in the dry season could increase. Trees are known to increase soil porosity and soil organic carbon<sup>37</sup>. Therefore, tree restoration, especially in treeless regions, promotes the infiltration capacity and the soil water storage capacity and reduces the

overland flow<sup>6,38–40</sup>. After tree restoration, the soils could thus potentially store more water, which would slowly be released during the dry season<sup>35</sup>. The true impact of tree restoration on water availability in the water-scarce regions may thus not be necessarily negative, and the impact depends on a combination of various aspects with high seasonal variability.

### Discussion and conclusions

The presented results are calculated using state-of-the-art data and methods, but several feedbacks and processes are not included in the analyses. Our approach does not consider the potential impacts of increased tree cover on atmospheric circulation and land–atmosphere interactions. Tree restoration could locally enhance convergence, cloud cover and precipitation and change the travelling direction and distance of atmospheric moisture<sup>18,41–43</sup>. Research suggests that forests could even impact large-scale wind patterns and draw atmospheric moisture from the oceans to the continents<sup>44,45</sup>, although the importance of this effect is still debated. These different feedbacks are poorly understood and difficult to incorporate in the present study because most evaporation–recycling models rely on meteorological reanalysis data, which are valid only under current land-cover conditions. The land–atmosphere interactions and potential changes in atmospheric circulation could impact the exact location and magnitude of increased precipitation. These processes could partly, but not fully, compensate for the enhanced evaporation, and this is unlikely to affect the main results of this study. In addition to data-driven studies, coupled land surface models have been used to reconstruct the effects of land-cover change on water availability<sup>46,47</sup>. Because of the large number of model parameters and feedbacks, their estimates of local impacts may be less constrained by observations and therefore more uncertain.

Furthermore, this study presents the impact of tree restoration under current climate conditions. However, global warming, and the tree restoration itself, will shift temperature and precipitation patterns<sup>48,49</sup>, and these are not considered in our analyses. Higher temperatures could reduce the global tree-restoration potential by 25% towards 2050<sup>2</sup>. Furthermore, higher temperatures will increase the potential evaporation and annual precipitation<sup>50</sup>, which causes a vertical shift in the Budyko framework (Extended Data Fig. 1b). Climate warming will impact the atmosphere’s dynamics, which will possibly result in a poleward shift of the Hadley cells and storm

tracks and a shift in magnitude of the jet streams<sup>51–54</sup>. The shifting global circulation will impact the patterns and magnitude of evaporation recycling.

This study estimated the effects of global large-scale tree restoration on water fluxes, including evaporation recycling. The results show that tree restoration shifts water availability and streamflow at both local and continental scales and that the patterns of increasing and decreasing water availability are complex throughout the globe. Following tree restoration, the increased precipitation could increase water availability locally; however, we find a global net loss of water availability over the continents. These conclusions are consistent with other data-driven or model-based studies of the effects of land-cover change on water fluxes<sup>18,46</sup>. We stress that future tree-restoration strategies should consider the hydrological effects. Smart tree-restoration strategies are necessary to secure the water supply locally and remotely or enhance the water supply in water-scarce regions.

### Online content

Any methods, additional references, Nature Research reporting summaries, source data, extended data, supplementary information, acknowledgements, peer review information; details of author contributions and competing interests; and statements of data and code availability are available at <https://doi.org/10.1038/s41561-022-00935-0>.

Received: 3 October 2021; Accepted: 23 March 2022;

Published online: 11 May 2022

### References

- Griscom, B. W. et al. Natural climate solutions. *Proc. Natl Acad. Sci. USA* **114**, 11645–11650 (2017).
- Bastin, J.-F. et al. The global tree restoration potential. *Science* **365**, 76–79 (2019).
- Land Restoration for Achieving the Sustainable Development Goals* (International Resource Panel, 2019).
- Wang-Erlandsson, L. et al. Remote land use impacts on river flows through atmospheric teleconnections. *Hydrol. Earth Syst. Sci.* **22**, 4311–4328 (2018).
- Seijger, C., Kleinschmit, D., Schmidt-Vogt, D., Mehmood-Ul-Hassan, M. & Martius, C. Water and sectoral policies in agriculture–forest frontiers: an expanded interdisciplinary research approach. *Ambio* **50**, 2311–2321 (2021).
- Ellison, D. *Forests and Water Background Analytical Study 2* (UN Forum on Forests, 2018).
- Brown, A. E., Zhang, L., McMahon, T. A., Western, A. W. & Vertessy, R. A. A review of paired catchment studies for determining changes in water yield resulting from alterations in vegetation. *J. Hydrol.* **310**, 28–61 (2005).
- Bosch, J. M. & Hewlett, J. D. A review of catchment experiments to determine the effect of vegetation changes on water yield and evapotranspiration. *J. Hydrol.* **55**, 3–23 (1982).
- Farley, K. A., Jobbágy, E. G. & Jackson, R. B. Effects of afforestation on water yield: a global synthesis with implications for policy. *Glob. Change Biol.* **11**, 1565–1576 (2005).
- Jackson, R. B. et al. Trading water for carbon with biological carbon sequestration. *Science* **310**, 1944–1947 (2005).
- Zhang, L., Dawes, W. R. & Walker, G. R. Response of mean annual evapotranspiration to vegetation changes at catchment scale. *Water Resour. Res.* **37**, 701–708 (2001).
- Filoso, S., Bezerra, M. O., Weiss, K. C. B. & Palmer, M. A. Impacts of forest restoration on water yield: a systematic review. *PLoS ONE* **12**, e0183210 (2017).
- Ning, T., Li, Z., Feng, Q., Chen, W. & Li, Z. Effects of forest cover change on catchment evapotranspiration variation in China. *Hydrol. Process.* **34**, 2219–2228 (2020).
- Sun, G. et al. Potential water yield reduction due to forestation across China. *J. Hydrol.* **328**, 548–558 (2006).
- Huxman, T. E. et al. Ecohydrological implications of woody plant encroachment. *Ecology* **86**, 308–319 (2005).
- Ellison, D., Futter, M. N. & Bishop, K. On the forest cover–water yield debate: from demand- to supply-side thinking. *Glob. Change Biol.* **18**, 806–820 (2012).
- Spracklen, D. V., Arnold, S. R. & Taylor, C. M. Observations of increased tropical rainfall preceded by air passage over forests. *Nature* **489**, 282–285 (2012).
- Meier, R. et al. Empirical estimate of forestation-induced precipitation changes in Europe. *Nat. Geosci.* **14**, 473–478 (2021).
- Keys, P. W., Wang-Erlandsson, L. & Gordon, L. J. Revealing invisible water: moisture recycling as an ecosystem service. *PLoS ONE* **11**, e0151993 (2016).
- Lawrence, D. & Vandecar, K. Effects of tropical deforestation on climate and agriculture. *Nat. Clim. Change* **5**, 27–36 (2015).
- Li, Y. et al. Divergent hydrological response to large-scale afforestation and vegetation greening in China. *Sci. Adv.* **4**, eaar4182 (2018).
- te Wierik, S. A., Cammeraat, E. L. H., Gupta, J. & Artzy-Randrup, Y. A. Reviewing the impact of land use and land-use change on moisture recycling and precipitation patterns. *Water Resour. Res.* **57**, e2020WR029234 (2021).
- Tuinenburg, O. A., Theeuwens, J. J. E. & Staal, A. High-resolution global atmospheric moisture connections from evaporation to precipitation. *Earth Syst. Sci. Data* **12**, 3177–3188 (2020).
- Zhang, L. et al. A rational function approach for estimating mean annual evapotranspiration. *Water Resour. Res.* **40**, W02502 (2004).
- Oudin, L., Andréassian, V., Lerat, J. & Michel, C. Has land cover a significant impact on mean annual streamflow? An international assessment using 1508 catchments. *J. Hydrol.* **357**, 303–316 (2008).
- Zhou, S., Yu, B., Huang, Y. & Wang, G. The complementary relationship and generation of the Budyko functions. *Geophys. Res. Lett.* **42**, 1781–1790 (2015).
- Teuling, A. J. et al. Climate change, reforestation/afforestation, and urbanization impacts on evapotranspiration and streamflow in Europe. *Hydrol. Earth Syst. Sci.* **23**, 3631–3652 (2019).
- Tuinenburg, O. A., Theeuwens, J. J. E. & Staal, A. *Global Evaporation to Precipitation Flows Obtained with Lagrangian Atmospheric Moisture Tracking* (Pangaea, 2020); <https://doi.org/10.1594/PANGAEA.912710>
- Tuinenburg, O. A. & Staal, A. Tracking the global flows of atmospheric moisture and associated uncertainties. *Hydrol. Earth Syst. Sci.* **24**, 2419–2435 (2020).
- In-Situ River Discharge Data* (GRDC, accessed 19 April 2021); <https://www.bafg.de/GRDC>
- Lehner, B., Verdin, K. & Jarvis, A. New global hydrography derived from spaceborne elevation data. *Eos* **89**, 93–94 (2008).
- Van Der Ent, R. J. & Savenije, H. H. G. Length and time scales of atmospheric moisture recycling. *Atmos. Chem. Phys.* **11**, 1853–1863 (2011).
- Roebroek, C. T. J., Melsen, L. A., Hoek van Dijke, A. J., Fan, Y. & Teuling, A. J. Global distribution of hydrologic controls on forest growth. *Hydrol. Earth Syst. Sci.* **24**, 4625–4639 (2020).
- Mekonnen, M. M. & Hoekstra, A. Y. Four billion people facing severe water scarcity. *Sci. Adv.* **2**, e1500323 (2016).
- Ellison, D., Wang-Erlandsson, L., Van Der Ent, R. J. & Noordwijk, M. V. Upwind forests: managing moisture recycling for nature-based resilience. *Unasylva* **70**, 14–26 (2019).
- van der Ent, R. J., Savenije, H. H. G., Schaeffli, B. & Steele-Dunne, S. C. Origin and fate of atmospheric moisture over continents. *Water Resour. Res.* **46**, W09525 (2010).
- Lal, R. Deforestation and land-use effects on soil degradation and rehabilitation in western Nigeria. I. Soil physical and hydrological properties. *Land Degrad. Dev.* **7**, 19–45 (1996).
- Ellison, D. et al. Trees, forests and water: cool insights for a hot world. *Glob. Environ. Change* **43**, 51–61 (2017).
- Bargués Tobella, A. et al. The effect of trees on preferential flow and soil infiltrability in an agroforestry parkland in semiarid Burkina Faso. *Water Resour. Res.* **50**, 3342–3354 (2014).
- Ilstedt, U. et al. Intermediate tree cover can maximize groundwater recharge in the seasonally dry tropics. *Sci. Rep.* **6**, 21930 (2016).
- Spracklen, D. V., Baker, J. C. A., Garcia-Carreras, L. & Marsham, J. H. The effects of tropical vegetation on rainfall. *Annu. Rev. Env. Resour.* **43**, 193–218 (2018).
- Ellison, D. & Ellis, E. *Forest Cover, Windspeed, and Precipitation: A South American Case Study of the Impact of Forest Ecosystems on Wind and Rainfall Patterns* EGU2020-22235 (EGU General Assembly 2020); <https://doi.org/10.5194/egusphere-egu2020-22235>
- Xu, R. et al. Contrasting impacts of forests on cloud cover based on satellite observations. *Nat. Commun.* **13**, 670 (2020).
- Makarieva, A. M. & Gorshkov, V. G. Biotic pump of atmospheric moisture as driver of the hydrological cycle on land. *Hydrol. Earth Syst. Sci.* **11**, 1013–1033 (2007).
- Sheil, D. & Murdiyoso, D. How forests attract rain: an examination of a new hypothesis. *BioScience* **59**, 341–347 (2009).
- Swann, A. L. S. et al. Continental-scale consequences of tree die-offs in North America: identifying where forest loss matters most. *Environ. Res. Lett.* **13**, 055014 (2018).
- Yosef, G. et al. Large-scale semi-arid afforestation can enhance precipitation and carbon sequestration potential. *Sci. Rep.* **8**, 996 (2018).
- Bonan, G. B. Forests and climate change: forcings, feedbacks, and the climate benefits of forests. *Science* **320**, 1444–1449 (2008).

49. Perugini, L. et al. Biophysical effects on temperature and precipitation due to land cover change. *Environ. Res. Lett.* **12**, 053002 (2017).
50. Konapala, G., Mishra, A. K., Wada, Y. & Mann, M. E. Climate change will affect global water availability through compounding changes in seasonal precipitation and evaporation. *Nat. Commun.* **11**, 3044 (2020).
51. Vecchi, G. A. et al. Weakening of tropical Pacific atmospheric circulation due to anthropogenic forcing. *Nature* **441**, 73–76 (2006).
52. Shaw, T. A. Mechanisms of future predicted changes in the zonal mean mid-latitude circulation. *Curr. Clim. Change Rep.* **5**, 345–357 (2019).
53. Jennifer, F. & Natasa, S. Evidence linking rapid Arctic warming to mid-latitude weather patterns. *Phil. Trans. R. Soc. A* **373**, 20140170 (2015).
54. Coumou, D., Di Capua, G., Vavrus, S., Wang, L. & Wang, S. The influence of Arctic amplification on mid-latitude summer circulation. *Nat. Commun.* **9**, 2959 (2018).

**Publisher's note** Springer Nature remains neutral with regard to jurisdictional claims in published maps and institutional affiliations.



**Open Access** This article is licensed under a Creative Commons Attribution 4.0 International License, which permits use, sharing, adaptation, distribution and reproduction in any medium or format, as long as you give appropriate credit to the original author(s) and the source, provide a link to the Creative Commons license, and indicate if changes were made. The images or other third party material in this article are included in the article's Creative Commons license, unless indicated otherwise in a credit line to the material. If material is not included in the article's Creative Commons license and your intended use is not permitted by statutory regulation or exceeds the permitted use, you will need to obtain permission directly from the copyright holder. To view a copy of this license, visit <http://creativecommons.org/licenses/by/4.0/>.

© The Author(s) 2022

## Methods

**Overview.** We calculate how a realistic scenario of large-scale tree restoration (restoring 900 million hectares of tree cover<sup>2</sup>) would impact the fluxes of evaporation ( $E$ ), precipitation ( $P$ ) and streamflow ( $Q$ ). The methodology includes four steps (Extended Data Table 1). (1) We use Budyko models to calculate  $E$  and  $Q$  before restoration. (2) We use Budyko models to calculate  $E$  and  $Q$  after restoration without evaporation recycling. (3) We use the UTrack dataset to calculate  $P$  after restoration on the basis of the increase in  $E$  calculated from steps 1 and 2. (4) We use Budyko models to calculate  $E$  and  $Q$  after restoration with evaporation recycling. The calculation of  $E$  and  $Q$  without evaporation recycling (step 2) is a local approach that assumes that evaporation increases with tree restoration but does not consider the effects of evaporation recycling. The calculation of  $E$  and  $Q$  with evaporation recycling (step 4) takes into account that the evaporated water partly recycles back to Earth's land surface and increases  $P$ .

**Input data to calculate  $E$  and  $Q$ .** The values of  $E$  and  $Q$  before tree restoration (step 1) are calculated using climatological  $P$  (Multi-Source Weighted-Ensemble Precipitation (MSWEP) v.2.8<sup>23</sup>), climatological potential evaporation (WorldClim v.2<sup>24</sup>) and current tree cover (Hansen tree cover v.1.7<sup>25</sup>). For  $E$  and  $Q$  after restoration (steps 2 and 4), we use tree cover after restoration (Hansen tree cover<sup>27</sup> + tree-restoration potential<sup>2</sup>, where we set the maximum tree cover after restoration to 1). The values of  $E$  and  $Q$  with evaporation recycling (step 4) are calculated using  $P$  after restoration (MSWEP  $P + P$  from evaporation recycling calculated in step 3). We assume that tree restoration does not affect potential evaporation. All input data were resampled to 0.00833° spatial resolution (~1 km at the Equator).

**Budyko models to calculate  $E$  and  $Q$ .** The values of  $E$  and  $Q$  before and after restoration are calculated using six different Budyko-type models<sup>11,24–27</sup> (Extended Data Table 2). These models reflect global annual patterns in  $P$  partitioning between  $E$  and  $Q$  (Extended Data Fig. 1). The general form of the equations is:

$$\frac{E}{P} = f\left(\frac{E_0}{P}, \omega\right),$$

where  $\frac{E}{P}$  is the fraction of precipitation partitioned into evaporation,  $\frac{E_0}{P}$  is the aridity index and  $\omega$  is a model parameter. Previous studies have suggested that the parameter  $\omega$  is closely related to vegetation type or vegetation coverage<sup>11</sup>. Six models were available in the literature that have a calibrated  $\omega$  parameter for forest and grassland cover. These models were calibrated using river-basin or lysimeter data from different climate zones. The parameter  $\omega_{\text{trees}}$  was calibrated with data from both natural forests (the major part of the data) and plantations. The vegetation parameter for grassland,  $\omega_{\text{grass}}$ , was calibrated using grassland data only or using both grassland and cropland data (Extended Data Table 3). The semi-empirical Budyko models reflect the yearly, catchment-integrated, effect of differences in interception, the plant available water, evaporation, the soil water storage capacity and the energy balance between grassland and forest.

For each of the six Budyko models,  $E$  and  $Q$  before and after restoration (without and with evaporation recycling) are calculated as:

$$E = E_{\text{trees}} \times \text{TC} + E_{\text{grass}} \times \text{NTC} \quad (\text{mm yr}^{-1}),$$

$$Q = Q_{\text{trees}} \times \text{TC} + Q_{\text{grass}} \times \text{NTC} \quad (\text{mm yr}^{-1}),$$

where  $E_{\text{trees}}$  and  $Q_{\text{trees}}$  are  $E$  and  $Q$  calculated for trees, TC is the tree cover,  $E_{\text{grass}}$  and  $Q_{\text{grass}}$  are  $E$  and  $Q$  calculated for grassland and NTC is the no tree cover, where:

$$\text{NTC} = 1 - \text{TC}.$$

NTC, thus, includes, among others, bare land, shrubland and built-up area. Evaporation from these land-cover types is different from evaporation from grassland and cropland. We expect that these differences are negligible because bare land is generally very arid, where  $E$  is close to zero (both the Budyko  $E$  and true  $E$ ), and built-up area has a limited extent. The Budyko vegetation parameters for shrubland (when calculated) closely resemble the parameters for grassland and cropland<sup>25,26</sup>.

Mean yearly  $Q$  before restoration was validated against streamflow data for 19 river basins (Fig. 1b). These 19 river basins are of the studied basins for which streamflow measurements and the river-basin outline were available in the Global Runoff Data Centre (GRDC) dataset<sup>30</sup>.

The changes in  $E$  and  $Q$  were calculated from the differences in  $E$  and  $Q$  before and after restoration. The results were resampled to 0.5° spatial resolution for the calculation of evaporation recycling.

**Evaporation recycling—calculation of precipitation.** We used the UTrack dataset<sup>23,28</sup> of global atmospheric moisture recycling (at 0.5° spatial resolution) to calculate where the additional evaporated water from restored trees would rain out ( $P$  after restoration in step 3). The UTrack dataset was created using

the state-of-the-art Lagrangian moisture-tracking model UTrack<sup>29</sup>. The dataset presents the monthly climatological mean evaporation recycling for each pixel. We aggregated the dataset's monthly mean evaporation recycling to yearly mean evaporation recycling to be able to combine it with the yearly Budyko models. This yearly aggregation of the UTrack dataset ignores the seasonality in direction and magnitude of atmospheric moisture transport that exists in some regions<sup>18,28</sup>. This aggregation was preferred above a disaggregation of the Budyko results because the Budyko model assumes zero change in water storage and can therefore be applied only on a multi-year mean timescale. Restoring tree cover could increase soil storage capacity and increase dry-season water availability<sup>38</sup>. Thus the Budyko models cannot be used to calculate evaporation at a monthly timescale. As a comparison, evaporation recycling was also calculated using a monthly time step for the river basins of the Mississippi, Orange and Ganges–Brahmaputra (Extended Data Fig. 2). When using the monthly time step, the total yearly evaporation is disaggregated over 12 months relative to the magnitude of evaporation for each month in the European Centre for Medium-Range Weather Forecasts Reanalysis v.5 data<sup>58</sup>. The monthly and yearly calculations have similar patterns and values, but there are differences of up to 1 mm yr<sup>-1</sup>.

In our approach, we assume that increased evaporation will amplify the current evaporation-recycling patterns. It is commonly assumed that land-cover change impacts evaporation recycling (patterns), but the effects of land-cover change on evaporation-recycling processes are poorly understood and difficult to determine<sup>41</sup>. There is currently no possibility to include these processes at high resolution at global scale, and therefore we use the UTrack dataset as the best available option.

## Data availability

The datasets for conducting the analysis presented here are available from the dataset of the global tree-restoration potential (<https://doi.org/10.1126/science.aax0848>, available on request), WorldClim dataset of potential evaporation (<https://doi.org/10.6084/m9.figshare.7504448.v3>), Utrack dataset for moisture recycling (<https://doi.org/10.1594/PANGAEA.912710>), MSWEP dataset for precipitation (<http://www.gloh2o.org/mswep/>, available on request), GRDC dataset for streamflow (<https://www.bafg.de/GRDC>) and HydroSHEDS database for the river basin outlines (<https://www.hydrosheds.org/products/hydrobasins>). The calculated evaporation and streamflow before restoration and changes in evaporation, streamflow and precipitation can be downloaded from <https://figshare.com/s/7e2e8d6064e745697f3e> (Name: ET\_Q\_P\_change\_tree\_restoration).

## References

- Beck, H. E. et al. MSWEP V2 global 3-hourly 0.1° precipitation: methodology and quantitative assessment. *Bull. Am. Meteorol. Soc.* **100**, 473–500 (2019).
- Trabucco, A. & Zomer, R. J. Global Aridity Index and Potential Evapo-Transpiration (ET0) Climate Database v2. *Figshare* <https://doi.org/10.6084/m9.figshare.7504448.v3> (2018).
- Hansen, M. C. et al. High-resolution global maps of 21st-century forest cover change. *Science* **342**, 850–853 (2013).
- Muñoz Sabater, J. ERA5-Land monthly averaged data from 1981 to present. *Copernicus* <https://doi.org/10.24381/cds.68d2bb30> (accessed 15 January 2020).
- Budyko, M. I. *Climate and Life* (Academic Press, 1974).
- Loveland, T. R. et al. Development of a global land cover characteristics database and IGBP DISCover from 1 km AVHRR data. *Int. J. Remote Sens.* **21**, 1303–1330 (2000).

## Acknowledgements

This study was supported by the Luxembourg National Research Fund (FNR) (PRIDE15/10623093/HYDROCSI) (A.J.H.v.D., K.M., M.M., M.S.). We thank D. Ellison for his useful feedback on a draft version of the manuscript.

## Author contributions

A.J.T. and A.J.H.v.D. conceived the idea of the study. A.J.H.v.D., A.J.T., I.B. and K.M. developed the methodology. A.J.H.v.D. carried out the analysis and wrote the first draft. All authors interpreted the results, contributed to the discussion and were involved in writing the final paper.

## Competing interests

The authors declare no competing interests.

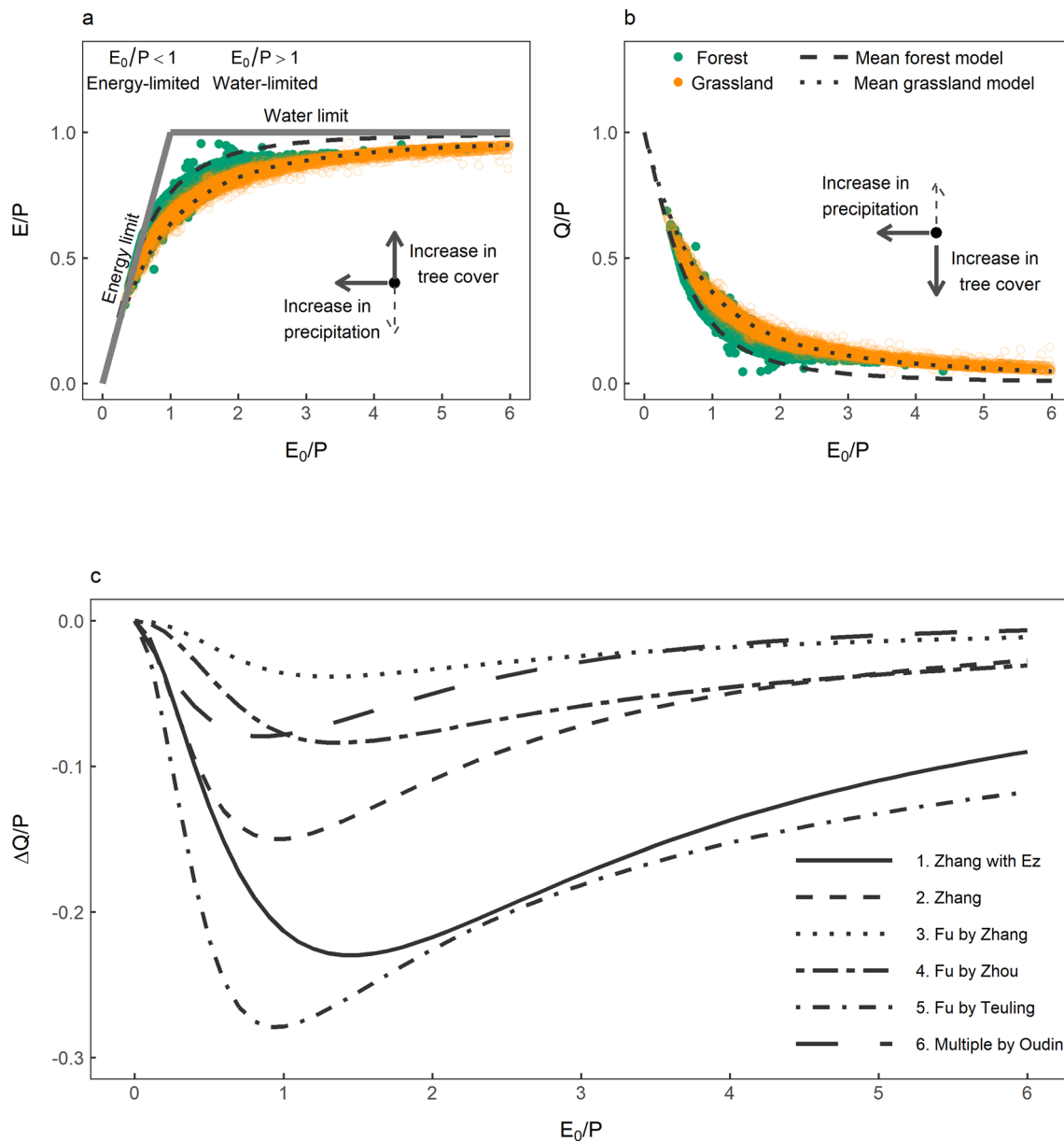
## Additional information

**Extended data** is available for this paper at <https://doi.org/10.1038/s41561-022-00935-0>.

**Correspondence and requests for materials** should be addressed to Anne J. Hoek van Dijke or Adriaan J. Teuling.

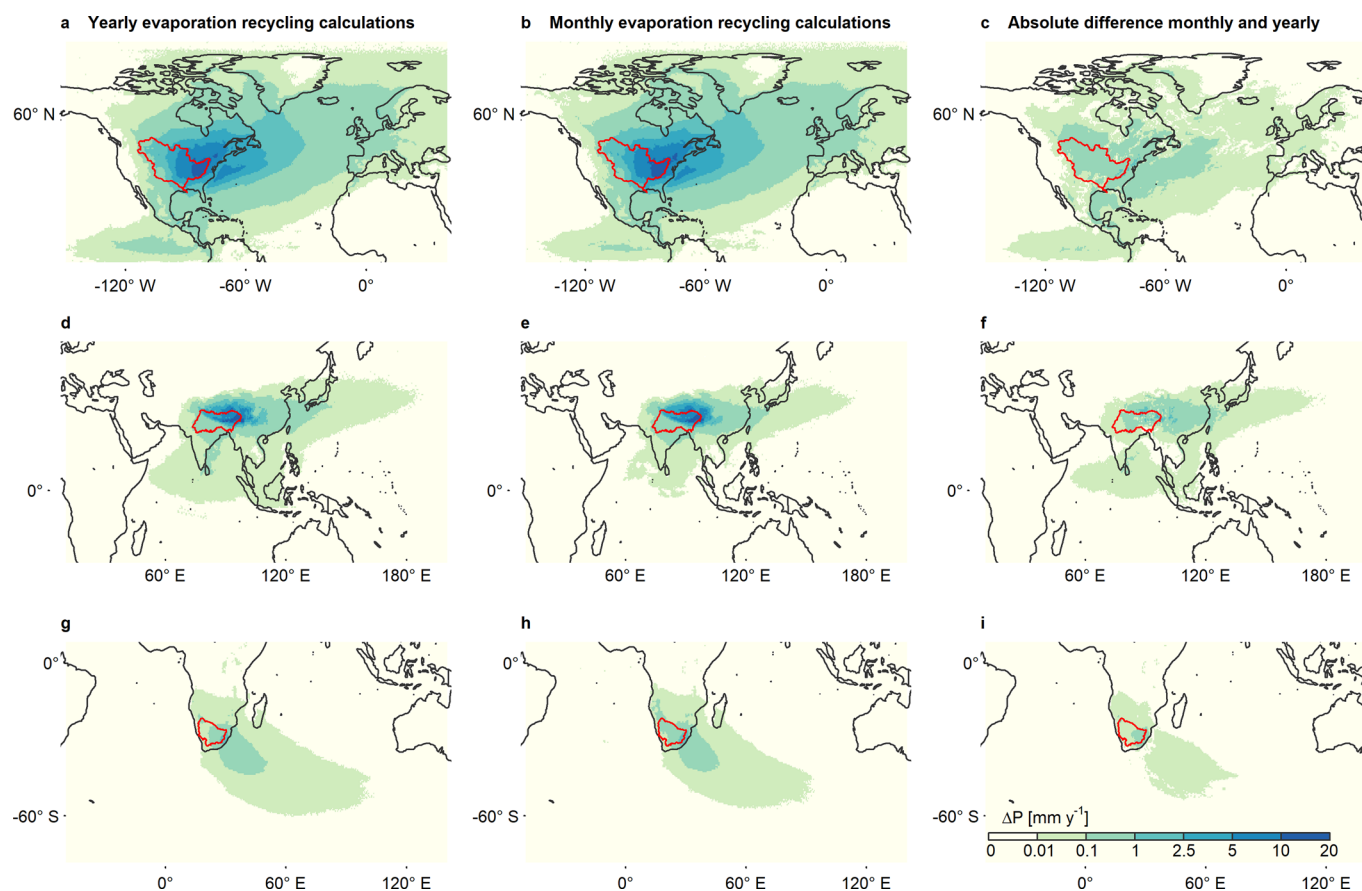
**Peer review information** *Nature Geoscience* thanks the anonymous reviewers for their contribution to the peer review of this work. Primary Handling Editor: Kyle Frischkorn and Tom Richardson, in collaboration with the *Nature Geoscience* team.

**Reprints and permissions information** is available at [www.nature.com/reprints](http://www.nature.com/reprints).

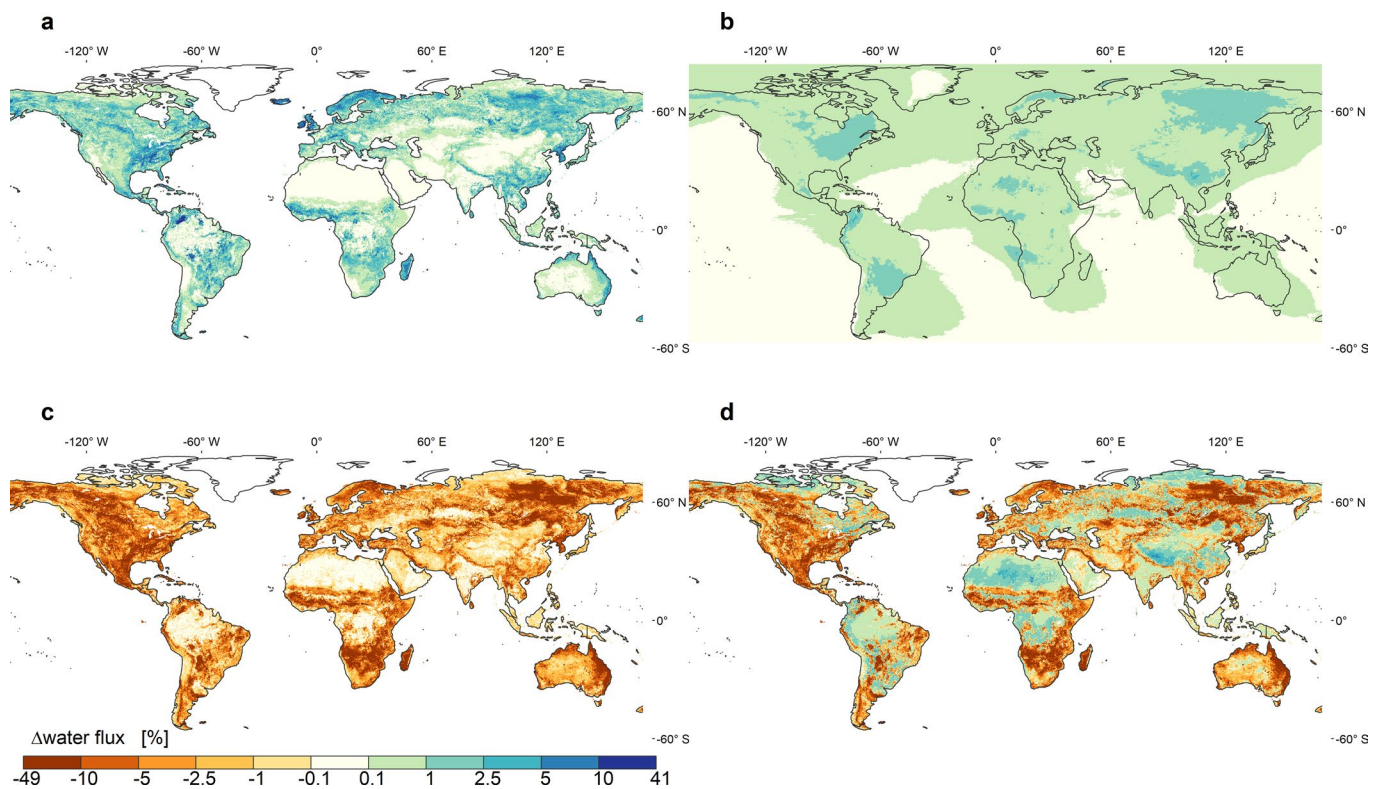


**Extended Data Fig. 1 | The Budyko framework.** The Budyko framework<sup>59</sup> parameterizes how the long-term aridity  $E_0/P$  (potential evaporation over precipitation ratio) determines the partitioning of precipitation into evaporation and streamflow. (a) displays the evaporation over precipitation ratio  $E/P$ , while (b) displays the streamflow over precipitation ratio  $Q/P$ . The dots display the range of values found in our study for grassland and forest (land-cover based on the IGBP dataset<sup>60</sup>). The lines represent the mean grassland and forest  $E/P$  and  $Q/P$ . The arrows show the direction of movement in the Budyko space for an increase in tree cover (which results in a higher  $E/P$  and lower  $Q/P$ ) and an increase in precipitation as a consequence of evaporation recycling (which results in a lower  $E_0/P$  and possibly a lower  $E/P$  and higher  $Q/P$ ). (c) displays the difference in  $Q/P$  between forest and grassland for the six different Budyko models. The numbers refer to the models in Extended Data Table 3.





**Extended Data Fig. 2 | Difference between yearly and monthly calculation of evaporation recycling from three river basins.** In our study, we present the results based on a yearly calculation of evaporation recycling. This figure displays the difference between the applied yearly calculation and a monthly calculation of evaporation recycling. For the yearly calculation, the monthly evaporation recycling from the UTrack dataset is aggregated to yearly evaporation recycling. For the monthly calculation, the increase in evaporation (from Budyko) is disaggregated over twelve months, relative to the local monthly evaporation from the ERA5-reanalysis product<sup>58</sup>. Both the yearly and the monthly calculation in this figure display the yearly aggregated evaporation recycling. The figures display the increase in precipitation following a tree-restoration induced increase in evaporation from three different river basins: (a-c) Mississippi basin, (d-f) Ganges-Brahmaputra basin, and (g-i) Orange basin. (a, d, and g) display the yearly calculation, (b, e, and h) display the monthly calculation, and (c, f, and i) display the absolute difference between the monthly and yearly calculation.



**Extended Data Fig. 3 | Difference between yearly and monthly calculation of evaporation recycling from three river basins.** (a-d) show the relative changes in water fluxes after forest restoration: change in (a) evaporation, (b) precipitation, (c) streamflow without evaporation recycling, and (d) streamflow with evaporation recycling. The maps display the 0.1° mean values, except for (b), which displays the 0.5° mean value.

**Extended Data Table 1 | The four steps applied to calculate the change in evaporation (E), precipitation (P) and streamflow (Q) without and with evaporation recycling**

| Step | Model / Dataset                     | Input evaporation ( $E$ )                             | Input potential evaporation ( $E_0$ )  | Input precipitation (P)              | Input tree cover                            | Output  |
|------|-------------------------------------|---|--|--------------------------------------|---|---|
| 1    | 6 Budyko models <sup>11,24-27</sup> |   | $E_0$ before restoration <sup>56</sup> | $P$ before restoration <sup>55</sup> | tree cover before restoration <sup>57</sup> | E and Q before restoration                              |
| 2    | 6 Budyko models                     |   | $E_0$ before restoration               | $P$ before restoration               | tree cover after restoration*               | E and Q after restoration without evaporation recycling |
| 3    | UTrack dataset <sup>23,28</sup>     | $\Delta E$ without evaporation recycling (step 1 + 2) |  | -                                    | -   | Increase in P   |
| 4    | 6 Budyko models                     |   | $E_0$ before restoration               | $P$ after restoration** (step 3)     | tree cover after restoration*               | E and Q after restoration with evaporation recycling    |

\* Tree cover after restoration is calculated from tree cover before restoration<sup>57</sup> + the tree restoration potential<sup>2</sup>.

\*\* P after restoration is calculated from P before restoration + increase in P (step 3).

**Extended Data Table 2 | The six Budyko-models that are used to calculate evaporation (E) and streamflow (Q) from precipitation (P) and potential evaporation (E<sub>0</sub>). Streamflow Q is calculated as:  $\frac{Q}{P} = 1 - \frac{E}{P}$**

| Model | Functional form*   | Calibrated $\omega$                                  | Details  |
|-------|--|--|--|
| 1     | $\frac{E}{P} = \frac{1 + \omega \frac{E_0}{P}}{1 + \omega \frac{E_0}{P} + \frac{P}{E_0}}$  | $\omega_{grass} = 0.5$<br>$\omega_{trees} = 2$       | Model developed and calibrated by Zhang, et al. <sup>11</sup> . Calibrated using 240 global river basins. $\omega_{trees}$ is calculated using natural and plantations data, and $\omega_{grass}$ is calibrated using grassland and cropland data.   |
| 2     | $\frac{E}{P} = \frac{1 + \omega \frac{E_z}{P}}{1 + \omega \frac{E_z}{P} + \frac{P}{E_z}}$  | $\omega_{grass} = 0.5$<br>$\omega_{trees} = 2$       | As Model 1 <sup>11</sup> . E <sub>0</sub> is also calibrated (E <sub>z</sub> ).<br>E <sub>z, grass</sub> = 1100, E <sub>z, trees</sub> = 1410  |
| 3     | $\frac{E}{P} = 1 + \frac{E_0}{P} - \left(1 + \left(\frac{E_0}{P}\right)^\omega\right)^{\frac{1}{\omega}}$                                | $\omega_{grass} = 2.55$<br>$\omega_{trees} = 2.84$   | Model developed by Fu in 1981, calibrated by Zhang, et al. <sup>24</sup> . Calibrated based on 200 Australian and 270 worldwide river basins. $\omega_{trees}$ and $\omega_{grass}$ are calibrated using river basins >75% forest and grassland cover.   |
| 4     | $\frac{E}{P} = 1 + \frac{E_0}{P} - \left(1 + \left(\frac{E_0}{P}\right)^\omega\right)^{\frac{1}{\omega}}$                                | $\omega_{grass} = 2.28$<br>$\omega_{trees} = 2.83$   | Model developed by Fu in 1981 <sup>24</sup> , calibrated by Zhou, et al. <sup>26</sup> . Calibrated with 1420 river basins with forest ( $\omega_{forest}$ ), and grassland and cropland ( $\omega_{grass}$ ) cover.   |
| 5     | $\frac{E}{P} = 1 + \frac{aE_0}{P} - \left(1 + \left(\frac{aE_0}{P}\right)^\omega\right)^{\frac{1}{\omega}}$                              | $\omega_{grass} = 1.7$<br>$\omega_{trees} = 3.1$     | Model by Fu 1981 <sup>24</sup> , calibrated by Teuling, et al. <sup>27</sup> . Calibrated based on European Lysimeter data. Teuling, et al. <sup>27</sup> introduced the adjusted potential evaporation (aE <sub>0</sub> = 1.6E <sub>0</sub> ) to account for lysimeter observations above the energy line.                            |
| a)    | $\frac{E}{P} = 1 - \exp\left(-\frac{\omega E_0}{P}\right)$   | $\omega_{grass} = 0.977$<br>$\omega_{trees} = 1.248$ | Mean E calculated from five Budyko equations of: a) Schreiber, b) Ol'DeKop, c) Turc, d) Budyko, and e) Zhang, Oudin, et al. <sup>25</sup> introduced $\omega$ in these equations to capture the vegetation effects. The formulas are calibrated using data from 1508 river basins in United States, United Kingdom, Sweden and France. |
| b)    | $\frac{E}{P} = \omega \frac{E_0}{P} \tanh\left(\left(\omega \frac{E_0}{P}\right)^{-1}\right)$  | $\omega_{grass} = 0.767$<br>$\omega_{trees} = 0.91$  |  |
| c)    | $\frac{E}{P} = \frac{1}{\left(1 + \left(\omega \frac{E_0}{P}\right)^{-2}\right)^{0.5}}$  | $\omega_{grass} = 0.831$<br>$\omega_{trees} = 1.025$ |  |
| d)    | $\frac{E}{P} = \left(\frac{E_0}{P}\right) \left(1 - \exp\left(-\omega \frac{E_0}{P}\right)\right) \tanh\left(\frac{P}{E_0}\right)^{0.5}$ | $\omega_{grass} = 0.762$<br>$\omega_{trees} = 1.125$ |  |
| e)    | $\frac{E}{P} = \frac{1 + \omega \frac{E_0}{P}}{1 + \omega \frac{E_0}{P} + \omega + \frac{P}{E_0}}$                                       | $\omega_{grass} = 0.682$<br>$\omega_{trees} = 1.404$ |  |

**Extended Data Table 3 | Impacts of large-scale tree restoration on evaporation (E), precipitation (P), and streamflow (Q) without and with evaporation recycling for 21 river basins**

| River basin        | Aridity |             | Tree                  |            |                       |            | $\Delta P$ basin recycling* | $\Delta Q \pm$ s.d. | $\Delta Q$ | $\Delta Q \pm$ s.d. | $\Delta Q$ | $\Delta Q$ |
|--------------------|---------|-------------|-----------------------|------------|-----------------------|------------|-----------------------------|---------------------|------------|---------------------|------------|------------|
|                    | Index   | restoration | $\Delta E \pm$ s.d.   | $\Delta E$ | $\Delta P \pm$ s.d.   | $\Delta P$ |                             | Without E           | Without E  | With E              | With E     | With E     |
|                    | (-)     | (%)         | (mm y <sup>-1</sup> ) | (%)        | (mm y <sup>-1</sup> ) | (%)        |                             | recycling           | recycling  | recycling           | recycling  | recycling  |
| Mackenzie          | 0.6     | 16.5        | 5.9 ± 3.7             | 1.7        | 3.5 ± 2.2             | 0.9        | 49.9                        | -5.9 ± 3.7          | -8.1       | -4.6 ± 3.8          | -6.4       | -281.1     |
| Colorado           | 0.2     | 9.9         | 2.2 ± 1.6             | 0.6        | 1.0 ± 0.7             | 0.3        | 23.6                        | -2.2 ± 1.6          | -6.4       | -2.0 ± 1.6          | -5.8       | -54.0      |
| Mississippi        | 0.6     | 22.9        | 17.8 ± 11.0           | 2.5        | 7.8 ± 4.9             | 1.0        | 58.6                        | -17.8 ± 11.0        | -8.5       | -14.1 ± 11.4        | -6.7       | -1607.7    |
| Orinoco            | 1.4     | 23.7        | 40.8 ± 26.7           | 3.6        | 16.1 ± 10.5           | 0.8        | 69.7                        | -40.8 ± 26.7        | -4.5       | -28.0 ± 27.7        | -3.2       | -941.4     |
| Amazon             | 1.6     | 12.0        | 10.8 ± 7.0            | 1.1        | 11.5 ± 7.5            | 0.6        | 46.7                        | -10.8 ± 7.0         | -1.8       | -1.9 ± 7.7          | -0.7       | -356.8     |
| LaPlata            | 0.8     | 21.4        | 15.7 ± 9.8            | 1.8        | 14.3 ± 9.0            | 1.2        | 45.6                        | -15.7 ± 9.8         | -5.6       | -7.9 ± 10.6         | -3.2       | -732.1     |
| Rhine              | 1.2     | 26.5        | 19.7 ± 12.7           | 3.1        | 7.2 ± 4.5             | 0.9        | 21.3                        | -19.7 ± 12.7        | -5.3       | -14.9 ± 13.3        | -3.9       | -103.4     |
| Danube             | 0.8     | 20.1        | 8.9 ± 5.6             | 1.4        | 6.4 ± 4.0             | 0.9        | 34.0                        | -8.9 ± 5.6          | -3.5       | -5.3 ± 6.1          | -1.9       | -156.5     |
| Niger              | 0.3     | 11.4        | 10.6 ± 6.8            | 1.1        | 6.7 ± 4.3             | 1.0        | 44.3                        | -10.6 ± 6.8         | -4.5       | -7.5 ± 7.0          | -2.8       | -613.3     |
| Nile               | 0.3     | 7.9         | 4.1 ± 2.7             | 0.5        | 4.0 ± 2.6             | 0.6        | 52.3                        | -4.1 ± 2.7          | -3.1       | -2.4 ± 2.8          | -2.1       | -263.7     |
| Congo              | 1.0     | 9.0         | 8.6 ± 5.4             | 0.9        | 9.5 ± 6.0             | 0.7        | 50.7                        | -8.6 ± 5.4          | -2.3       | -2.8 ± 6.0          | -0.9       | -340.2     |
| Zambezi            | 0.5     | 19.4        | 16.3 ± 10.7           | 2.2        | 7.5 ± 4.8             | 0.9        | 55.2                        | -16.3 ± 10.7        | -10.8      | -13.6 ± 10.6        | -9.2       | -670.8     |
| Orange             | 0.2     | 7.8         | 1.7 ± 1.3             | 0.4        | 2.2 ± 1.6             | 0.6        | 13.8                        | -1.7 ± 1.3          | -5.4       | -1.3 ± 1.3          | -4.2       | -43.2      |
| Volga              | 0.8     | 19.0        | 4.5 ± 2.7             | 1.0        | 3.8 ± 2.4             | 0.7        | 22.0                        | -4.5 ± 2.7          | -3.0       | -2.6 ± 3.0          | -1.6       | -132.6     |
| Euphrates-Tigris   | 0.2     | 10.2        | 1.6 ± 1.2             | 0.4        | 1.1 ± 0.7             | 0.3        | 17.3                        | -1.6 ± 1.2          | -3.9       | -1.3 ± 1.2          | -3.4       | -46.4      |
| Yenisei            | 0.8     | 17.7        | 6.5 ± 4.0             | 1.8        | 4.9 ± 3.0             | 1.1        | 42.7                        | -6.5 ± 4.0          | -7.2       | -4.2 ± 4.4          | -5.1       | -376.5     |
| Ganges-Brahmaputra | 0.8     | 12.1        | 8.5 ± 5.5             | 0.9        | 6.2 ± 4.0             | 1.7        | 53.6                        | -8.5 ± 5.6          | -1.7       | -4.7 ± 5.9          | -0.4       | -263.8     |
| Yangtze            | 1.0     | 15.7        | 10.2 ± 6.5            | 1.3        | 13.2 ± 8.4            | 1.3        | 32.6                        | -10.2 ± 6.5         | -2.5       | -1.7 ± 7.3          | -0.2       | -109.5     |
| Mekong             | 1.0     | 17.7        | 18.4 ± 11.5           | 1.7        | 7.6 ± 4.8             | 0.6        | 31.0                        | -18.4 ± 11.5        | -3.6       | -13.6 ± 12.0        | -2.6       | -435.7     |
| Kapuas             | 2.5     | 8.7         | 9.8 ± 6.9             | 0.7        | 7.7 ± 5.2             | 0.3        | 12.5                        | -9.8 ± 6.9          | -0.5       | -2.7 ± 7.1          | -0.1       | -9.7       |
| Murray-Darling     | 0.3     | 17.1        | 5.3 ± 3.6             | 1.0        | 1.6 ± 1.1             | 0.4        | 34.6                        | -5.3 ± 3.6          | -8.0       | -4.9 ± 3.6          | -7.3       | -177.7     |

\*  $\Delta P$  basin recycling is the percentage of  $\Delta P$  that had evaporated within the same river basin. Note that  $\Delta P$  basin recycling depends on the size and shape of the basin, and that the values cannot be compared between basins.

The standard deviation (s.d.) reflects the variation over the six different Budyko models.